98-613

Final Report

(January 1, 1998 to March 31, 1998)

DESIGN AND HARDWARE SPECIFICATIONS FOR A 500MHz BANDWIDTH ACOUSTO-OPTIC LPI RADAR CORRELATOR

for

Defence Research Establishment Ottawa(DREO)
Contract No. W7714-7-0118/001/SV
Scientific Authority: J.P.Y. Lee
Fax: (613)990-8401

by

V.M. Ristic
Fax: (416)485-0032

March, 1998

Executive Summary

Hardware and system specifications for design and realization of an AO processor for ESM applications are discussed and recommended. The processor is to cover 0.5 to 26.5 GHz band with special emphasis on extraction of the LPI radar signals. Further research efforts into the field of acousto-optic interaction, in presence of a high acoustic attenuation, are also recommended with a goal of further ameliorating the existing processor design.

Contents

1 Optical Processors, Correlation Architectures and Spectral Analysis 2

2 Design and Hardware Specifications 6

2.1 ESM Requirements 6

2.1.1 Technical Considerations Related to Tuners 6

2.1.2 The Delay Time of an AO Deflector 7

2.1.3 Detector Integration Time, LPI Radar PRF, Processing Gain, and Coherent and Incoherent Detection 12

2.2 In-Line (Multiplicative) Architecture 15

2.3 Hardware Specifications 16

2.3.1 AO Deflector, Acoustic Delay Line, and Delay Line RF Power Amplifier 16

2.3.2 Laser Diode, Intensity Modulation and Loaser Focussing Optics . . . 16

2.3.3 Pre-Detection Optics and CCD Array at the Time-Integrating Output 18

2.3.4 The Notching Adaptive Feedback Loop, Notch Filters, AGC and Space-Integrating Output 18

2.3.5 Auxiliary Electronics 19

3 Application of Designed Processor to Signals with Strong Doppler Effect 19

4 Conclusions and Recommendations 20

5 References 20

6 Appendix I 27

7 Appendix II 28

1 Optical Processors, Correlation Architectures and Spectral Analysis

In the past five decades of optical signal processing (OSP) many optical processors were developed [1-4]. In the 1950's coherent and incoherent Fourier processors were developed [5]. Concepts such as frequency-plane filtering of coherent images [7], VanderLugt filters [7], nonlinear filtering [8], and space-variant filtering [9] were established. Other processors [10,11] offered linear convolution by employing optical multiplication of translating images with spatial integration. This technique became very popular with acousto-optic (AO) modulators as one-dimensional (1-D) translating optical inputs [12]. In the 1960's and 1970's coherent processors received considerable attention primarily because of the Fourier transform capability and secondary because of high data rate parallel processing (which also applies to incoherent processing). The high-data rate of optical processors was the main justification for research in optical processors due to increasing competition from digital signal processing (DSP) electronics. The DSP has many advantages over OSP such as more general algorithm capability, ease of programmable modification, noise immunity, ease of data storage and manipulation, and environmental stability.

Today the OSP remains attractive for high data rates (Gflops to Tflops) and noise performance that cannot be met with DSP. A number of optical processors was developed for high data rates such as AO processors [13] and incoherent processors [11,14] that avoid noise problems associated with coherent light. Hybrid processors [15] that combine both, DSP and OSP, were also investigated (today it is realized that the vast majority of optical processors in use consists basically of 20-30% optical and 80-70% electronic hardware).

One of the most successful electrical/optical transducer with high data rates has been

the AO cell. The AO processors were first considered during 1950's [16,17]. The AO processors were used in correlators [18-21], phase array radars [22], ambiguity function processors [18,19], and spectrum analyzers [18,19].

The first optical 1-D and 2-D processors that have offered enhanced environmental stability are those devised by Kellman [19,23] in 1979 (optical processors, based on Kellman's work, are presently being seriously considered for LPI radar correlation purposes). It is well known that some optical processors (such as the Mach-Zehnder type) provide a number of useful functions [1] but are notoriously difficult to align, and are very sensitive to mechanical vibrations and air currents. By introducing an electronic reference signal into the AO cell Kellman has succeeded in producing a processor with considerable mechanical stability. However, the amount of electronics required to achieve this goal would, at least, force us to call this processor a hybrid. However, today it is customary to call them optical processors since the high data rates offered by them are presently unachievable with the DSP. Another important point is that acousto-optic is a natural fit [1,24] to the convolution or correlation application as well as to many others. In these applications, the required electronic back-up is reasonable. Outside these applications the harnessing of the acousto-optic technology may require such an extensive electronic back-up that other technologies should be considered.

Many optical processors are required to process broad-band signals (BBSs), with very low S/N ratios, in presence of strong narrow band interfering signals (NISs). This requires certain types of preprocessing, since for instance, in an AO processing correlator the NISs must be first excised before correlation of the BBSs is attempted [25]. In the beginning of 1980's, Erickson [26,27] carried out experimental and theoretical investigation of signal excision by using spatial filters in the spatial frequency plane. This was followed by the work of Lee et al. [28] who used a threshold detector array to control spatial light modulator

(SLM) in the spatial frequency plane. Roth [29] used a photodetector array to remove interfering signals. Anderson et al. [30] carried out excision using a GaAs photodetector array. An optical notching filter that uses a recursive technique, to increase notch depths, was reported by Brandsteller and Grieve [31]. Finally, Ward and VanderLugt [32] used an acousto-optic SLM to excise interfering signal in the spatial frequency plane. This was, in fact, the last attempt to use "optical spectrum analysis" for excision processing. Since 1992 leading researchers in the field of excision, being discouraged by inability of the present optics technology to produce an adequate optical excisor have turned their attention to the application of DSP to excision problems [33-37,25]. This approach brought success [36,25,37] to the problem of the NISs excision.

Recently, Riza [38-42] devised an interferometric time-integrating AO correlator that is inherently stable. It uses two AO cells to achieve the desired results. In our opinion, further evaluation of this processor is necessary in order to understand better all its features.

In the last two decades 2-D processors were also considered. Here problems associated with environmental stability are even more accentuated. For that reason only 2-D processors with electronic reference will be considered [23]. Consider a radar processor, such as a 2-D correlator, sometimes called a triple-product processor [43], which uses three input signals for multidimensional processing. This can be represented by triple-product integral [23]

$$\int_{-\infty}^{+\infty} f(t)g(t)h(t)dt \tag{1.1}$$

In a radar application a sample of the transmitted signal $s_1(t) = f(t)$, the return signal from the target delayed by time τ_1, and received by an antenna $s_2(t - \tau_1) = g(t)$, and the return signal delayed by time τ_2, received by a second antenna $s_3(t - \tau_2) = h(t)$ are used. The

delays τ_1 and τ_2 are both measured in respect to $s_1(t)$. From two separate sites in a bistatic geometry these delays can be used to determine the target's range.

In signal intercept applications, three non-colinear antennas are used to provide three signals to the correlator. All the received signals are unknown and are given by $s_1(t) = f(t)$, $s_2(t-\tau_1) = g(t)$ and $s_3(t-\tau_2) = h(t)$. Again, delays τ_1 and τ_2 are in respect to $s_1(t)$. This processor is used to determine AOA of the SOI in two planes.

By modifying the input signals the radar ambiguity function can also be generated with 2-D processors. An internally generated chrip signal is multiplied by a sample of the transmitted signal resulting in $f(t) = s_1(t)\exp(-j\pi t^2)$. The received signal is modelled by $g(t) = s_2(t-\tau_1)\exp(j2\pi\mu t)$, where the exponential function indicates the differential Doppler shift μ. A second internally generated chirp is used as a third input signal, $h(t) = \exp(-j\pi(t-\tau_2)^2]$, where the delay τ_2 can be varied by the user. By displaying correlation magnitude versus time, a peak will occur at $\tau_2 = \mu$. The position of the peak will reflect both relative motion and range of the target.

In signal intercept applications Wigner-Ville distribution function is sometimes needed. This correlation requires that a chirp signal is multiplied by one unknown input signal $f(t) = s_1(t)\exp(-j\pi t^2)$. The other signals are $g(t) = w(t)$, where $w(t)$ is a window function of finite length, and $h(t) = \exp[j\pi(t-\tau_2)^2]$ is the variable chirp delay similar to one used to determine the Doppler effect. The Wigner-Ville function provides a one-plane, short-time spectrum analysis of the received signal.

Since the pioneering work of Kellman [23], there has been few attempts to build and evaluate 2-D acousto-optic processors [44-48]. A consensus among researchers is that further technological advances are needed in the field of 2-D CCD arrays as well as in the area of AO devices for the 2-D optical processors to be seriously considered. The cost of the presently

available components is also often prohibitive.

2 Design and Hardware Specifications

2.1 ESM Requirements

Considerable efforts are being made in front-end hardware design of ESM systems to incorporate DSP as close as possible to the antenna (or other front end sensor), and then to extract signals of interest efficiently from the noise which is then followed up by sophisticated DSP techniques for spectrum analysis [49]. How the capture of multiple and simultaneous signals, that are of interest, is achieved makes a decisive impact on how the front-end is designed. It is important to remember that radar designers are increasingly using more sophisticated jam-resistant and covert forms of modulation, in particular, spread-spectrum signals. Spread-spectrum may also use spectral overlapping techniques such as code division multiple access (CDMA) which even confuses more an unauthorized receiver since similar looking signals share common bandwidth. Other modulation that may be in use is quadrature-amplitude modulation (QAM).

2.1.1 Technical Considerations Related to Tuners

The detection of multiple and simultaneous signal buried in noise, in our design, is achieved by using wideband tuners [50-52]. In order for the tuners to be able to detect signals with QAM they must have low phase noise [50,51]. The output of the wideband tuners can be digitized and various DSP techniques used for extraction of the signals from noise. However, in a dense radar signal environment, which requires rapid spectral analysis for detection, characterization, and identification of simultaneous multiple signals buried in noise the DSP

techniques, at present, are too slow. By far a better approach is to use AO processors, immediately after the tuners, and then to apply the DSP techniques.

2.1.2 The Delay Time of an AO Deflector

The delay (dwell) time T of an AO deflector together with the AO bandwidth B_{AO} determines the time-bandwidth product $T \cdot B_{AO}$ of the cell. Consider, for instance, the Brimrose [53] GaP AO deflector, GPD-1500-1000, with effective optical aperture, $T_{eff} = 0.167$ μs (this is the delay time over which the diffraction efficiency changes by 3 dB at the center frequency. Also note that the efficiency curve was not measured at the center frequency but at the low cutoff frequency $f_l^{AO} = 1$ GHz) and $B_{AO} = 1$ GHz thus giving us $T_{eff}B_{AO} = 167$. However, the full delay, i.e. maximum aperture, of the deflector is 1 μs long but the diffraction efficiency falls from 60% at $x = -L/2 = -3.125$ mm, see Fig. 1, at the transducer to approximately 1% at $x = L/2 = +3.125$ mm, at center frequency $f_0^{AO} = 1.5$ GHz. The time-bandwidth product equals to 167 distinct points (spots) in the image plane of the AO deflector that can be used to determine the shape of the envelope of the correlation signal.

Also the ratio of $B_{AO}/T_{eff}B_{AO}$ determines the resolution of the system. For instance, for $T_{eff} = 0.167$ and 0.4 μs the resolution is 6 MHz and 2.5 MHz per bin, respectively. The result of 2.5 MHz is acceptable while the 6 MHz one is not. Therefore, we will be adapting for our design the Brimrose AO deflector GPD-1500-1000 with $T_{eff} = 0.4$ μs, or $L = 2.53$ mm.

It is to be noted that the attenuation problem is a serious one and is of considerable interest in broadband signals. In what follows the severity of the problem is illustrated. This is followed by a novel idea, not described in the literature, of how to increase the time-bandwidth product by introducing predistortions into the deflector driver, Fig. 1. The

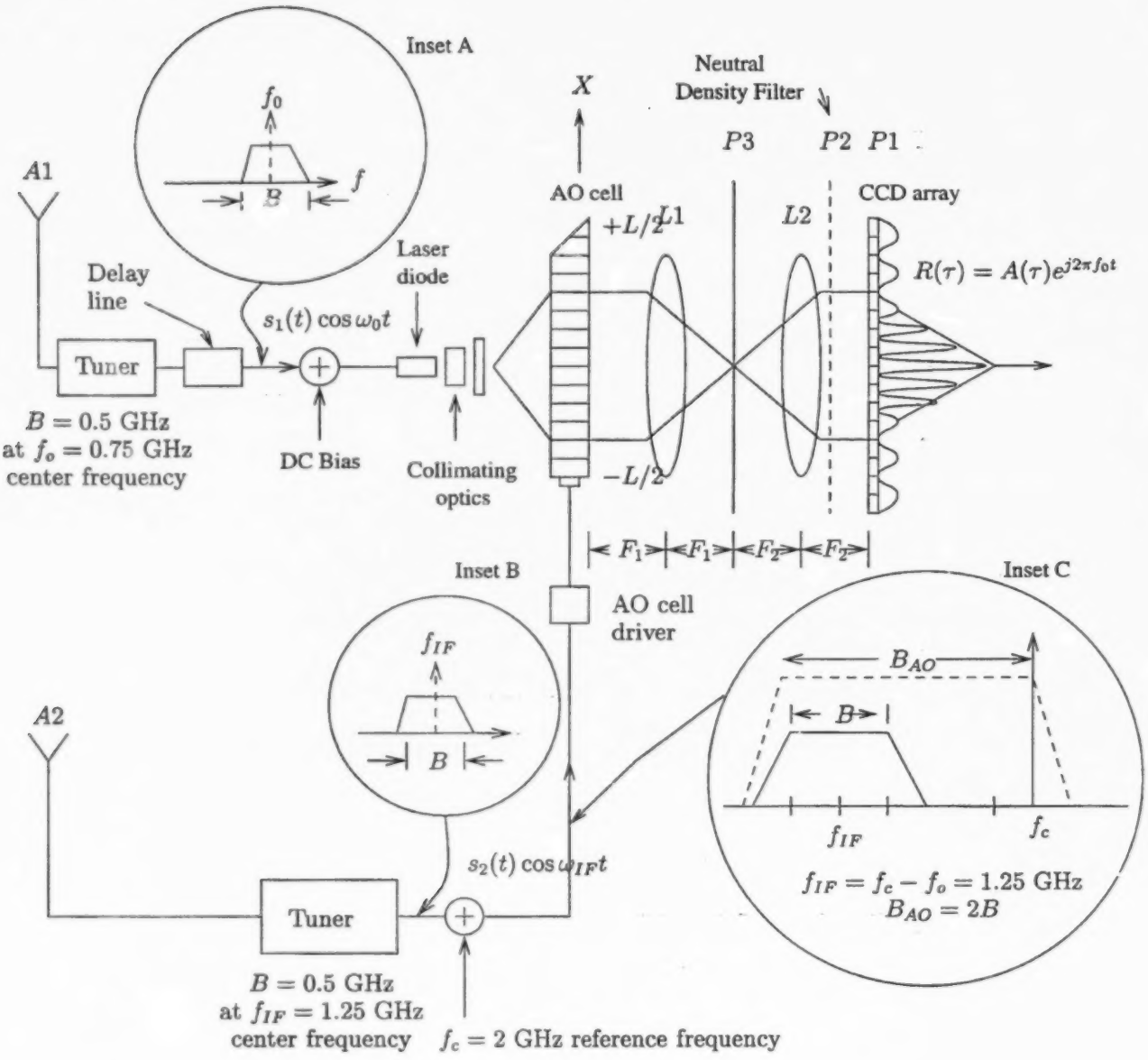

Figure 1: A time-integrating acousto-optic processor with multiplicative architecture

acoustic (frequency-dependent) attentuation factor [1] is given by

$$a_0(x,f) = \exp[-c(x+L/2)f^2], \quad |x| \le L/2 \tag{2.1}$$

where c is an attenuation constant, and $x = 0$ defines the center of the AO deflector, as shown in Fig. 1. Furthermore, $c = 0.23\Gamma/\text{s}$, where for GaP, $\Gamma = 3.80$ dB/(μs.GHz^2) and $v = 6.32$ km/s giving $c = 0.138$ dB/mm.GHz^2. THus,

$$a_0(-L/2,f) = 1 \quad \text{and} \quad a_0(+L/2,f) = \exp(-cLf^2) \tag{2.2}$$

the ratio of Eqs. (2.2) is

$$A(f) = 20\log\left[\frac{a_0(-L/2,f)}{a_0(+L/2,f)}\right] = -8.68cLf^2 \tag{2.3}$$

For the GaP AO deflector under consideration, at center frequency $f_0^{AO} = 1.5$ GHz, and full aperture of $l = 6.3$ mm of the ratio $A(1.5) = -17$ dB. Since we are dealing with broadband signals it is important to know how the AO processor distorts the signal before processing it. Thus, instead of finding the ratio $A(f)$ at the center frequency $f = 1.5$ GHz, which is highly misleading for broadband signals, let us find how the lowest frequency signals at $f_\ell^{AO} = 1$ GHz and the highest frequency $f_h^{AO} = 2$ GHz are distorted. From Eq. (2.3) it is found that $A(1) = -7.6$ dB and $A(2) = -30$ dB. Thus, if the full bandwidth is used the difference is attenuating factors at the band ends is 22.4 dB. Consider now an AO deflector with center frequency $f_0^{AO} = 3$ GHz, $BW = 2$ GHz, aperture $L = 3.15$ mm, $f_\ell^{AO} = 2$ GHz and $f_h^{AO} = 4$ GHz. The attenuation ratios at the band ends are $A'(2) = -15$ dB and $A'(4) = -60$ dB resulting in a difference of 45 dB.

An immediate partial remedy for this situation is the use of amplitude predistortion in the AO cell driver in order to compensate somehow for the attenuation effects. Furthermore, more fundamentally what is needed is a revisiting of the theory of the AO interaction with severe acoustic attenuation. Simultaneously computer modelling of the AO processor (with severe acoutic attenuation) should be pursued in order to find out how detection of broadband signals is affected by the attenuation.

At present, AO deflectors with $B_{AO} = 2$ GHz cannot be fully exploited due to high attenuation. If they could be fully exploited, for instance, in Kellman's 1-D time-integrating architecture, the available signal bandwidth would be $B = 1$ GHz and the ESM frequency band of 0.5 to 26.5 GHz could be covered, in principle, by 26 AO deflectors without need for wideband tuners. This, of course, would lead to a new architecture offering a *real-time* 100% interception of signals, and avoid distortion of signals introduced by the wideband tuners.

Returning to the idea of introducing predistortion into the deflector driver, it is to be noted, that, in present designs, both components of signal at f_ℓ and f_h produce the same amplitude at the transducer, $x = -L/2$, where $V_\ell = V_h$ are the relevant amplitudes, as shown in Fig. 2(a).

In this case, as the signal propagates through the AO deflector, *at all time* the low frequency components make larger contributions to the processing than the high frequency components. A better approach is shown in Fig. 2(b) where the amplitude of the low frequency components is decreased, so that in the first half of the aperture the amplitude of the high frequency components predominates, while in the second half of the aperture the low frequency components predominates. It is possible with this approach to increase T_{eff} while keeping distortions of the signal within reasonable limits. Predistortions should also be contemplated for the RF amplifier (not shown) feeding the acoustic delay line at the

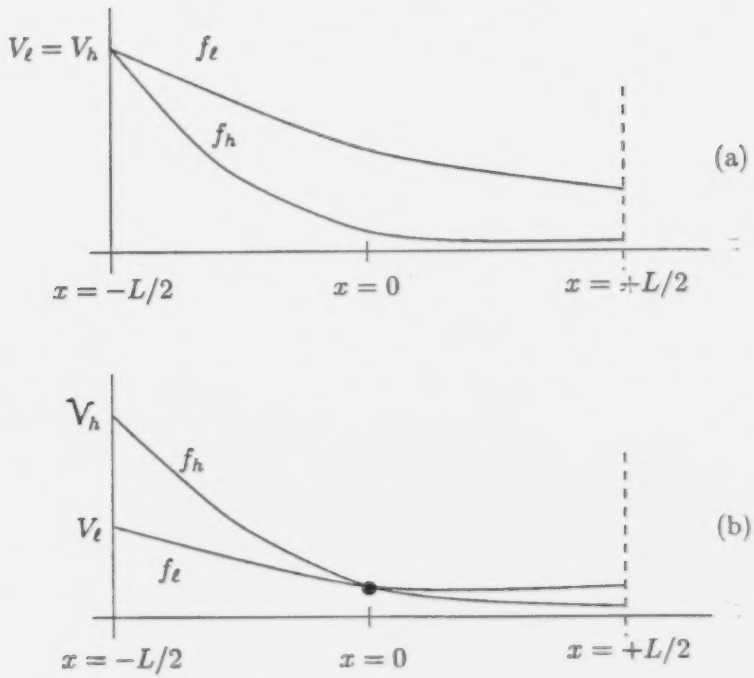

Figure 2: (a) A standard operation of the AO deflector and (b) operation with predistortion; V_ℓ and V_h, and f_ℓ and f_h are the low cuttoff and high cutoff voltages and frequencies of the signal band, respectively.

antennas input A_1 of Fig. 1.

With reference to Fig. 3 we end this section by stating the *specifications for the AO deflector:*

(a) AO bandwidth: 1 GHz

(b) Effective optical aperature: $T_{eff} = 0.4\ \mu$s

(c) Effective aperature (GaP): 2.53 mm

(d) Center frequency: 1.5 GHz

With reference to Fig. 1 and references [25,37] the *specifications for the system frequencies* are:

(e) Signal bandwidth: 0.5 GHz

(f) Signal IF frequency: $f_{IF} = 1.25$ GHz

(g) Electronic reference frequency: $f_c = f_h^{AO} = 2$ GHz

(h) Difference (offset) frequency: $f_0 = 0.75$ GHz

As far as tuners are concerned there is really only one choice [51]: Watkins-Johnson WJ-TN-170 receiver.

2.1.3 Detector Integration Time, LPI Radar PRF, Processing Gain, and Coherent and Incoherent Detection

It was shown [54], see also Appendix I, that the correlation signal at the detector plane, Fig. 1, of a time-integrated AO processor is given by

$$R'(\tau) = A(\tau)\cos[\alpha\pi f'\tau + \phi(\tau)], \qquad \tau = T/2 + x/v \tag{2.4}$$

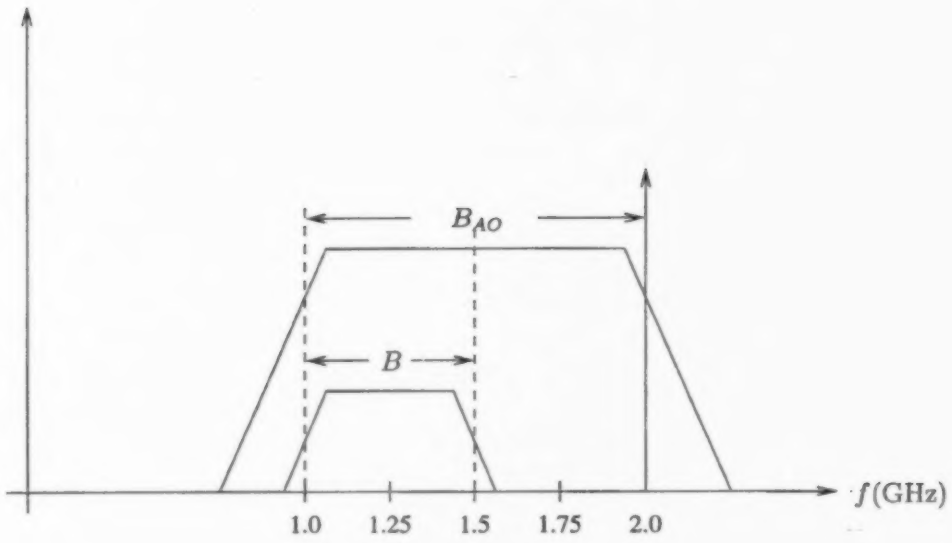

Figure 3: Frequency relationship in the AO processor: B_{AO} acousto-optic bandwidth, B signal bandwidth, the signal IF frequency $f_{IF} = 1.25$ GHz, the electronic reference frequency $f_c = 2$ GHz $= f_h^{AO}$ the upper cutoff frequency of the AO bandwidth, f_0 the difference (offset frequency), $f_0 = f_c - f_{IF} = 0.75$ GHz, the lower cutoff frequency f_ℓ of the signal spectrum is at 1 GHz, the upper cutoff frequency $f_h = 1.5$ GHz and the center frequency of the AO delay line is at $f_0^{AO} = 1.5$ GHz.

where the bias term has been neglected. The highest frequency in the correlated signal, Fig. 3, is $f' = f_h = 1.5$ GHz. To record this frequency, according to the sampling theorem, a pixel spacing equal to or less than $0.5/f'$ is needed. With an AO cell with effective aperture of $T = 0.4$ μs the number of pixels in the detector plane required should be 0.4 $\mu s f'/0.5 = 1200$. Assuming that the physical aperture of the detector equals that of the AO deflector, as it is the case in our design, the pixel spacing required would be 2.53 mm/1200 = 2 μm, a very difficult requirement especially if a high dynamic range (DR) is required. Fortunately, in the processor in Fig. 1, only the correlation signal envelope $A(\tau)$ in Eq. (2.4) needs to be detected. This reduces the data rate to something in between 1 and 20 MHz, which is primarily driven by radar PRF or the signal intercept TDOA resolution requirements. For instance, taking for the highest frequency of interest in the correlation envelope to be 50 MHz would result in the minimum number of pixels equal to 0.4 $\mu s \times 50$ MHz$/0.5 = 40$. Allowing for the oversampling, a good choice for the number of pixels would be in the 100-160 range. So the pixel spacing is not a problem. (Much more serious problems, as considered later, are the required large DR and large integration time T_i.) The DSP processors capable of handling 50 MHz bandwidth are available: a 1000 point complex FFT can be completed in time less than 65 μs [55]. The most critical aspect of the CCD detector array is, due to time-integrating nature of the processor, the detector integration time. The T_i is determined by the saturation voltage of the array V_{SAT}, while the detector peak-to-peak noise V_{PP} with V_{SAT} determines the detector dynamic range $DR = V_{SAT}/V_{PP}$. The detector integration time features prominently in the processor gain equation [25,37],

$$G_P \simeq (BT_i) \cdot \frac{T_i}{T_P} \qquad (2.5)$$

where $T_P = 1/PRF$ is the interval between the radar pulses and $T_i/T_P = N$, the number of radar pulses, and B is the signal bandwidth. The detector integration time required could be anywhere in 20 μs to 20 ms range with detector dynamic range of about 50 dB and the detector readout rate in the range from 0.5 MHz to 50 MHz. Note that for $T_i \equiv T_P$ in Eq. (2.5) the processor is no longer delivering time-integrating gain. Thus the lower limit of T_i determines the threshold of detection for low PRF radars. The higher limit of the detection integration time is determined by the saturation voltage of the array. Special arrays have been built to satisfy these requirements [56]. In Eq. (2.5) we have assumed a coherent detection. For incoherent detection the approximate processing gain would be given by

$$G'_P = (BT_i) \cdot \sqrt{\frac{T_i}{T_P}} \qquad (2.6)$$

which would reduce by half (in dB) the processing gain due to time integration.

2.2 In-Line (Multiplicative) Architecture

The in-line (multiplicative) architecture, Fig. 1, depicts the principal elements of the processor. Not shown are the notching adaptive feedback loop, the space-integrating output, the notch filters, and the acoustic delay line amplifier. The two feedback loops, shown in Fig. 4, connect the space-integrating output to NIS excision filter bank for *fast* detection and excision of NIS, and the time-integrating output to NIS excision filter bank for *slow* detection and excision of NIS. The NIS filter banks are placed immediately after tuners at inputs A_1 and A_2 in Fig. 1. Note that the fast feedback loop in Fig. 4 can be used, with appropriate modifications, for AGC by connecting it to AO deflector driver, or to acoustic delay line RF amplifier (not shown in Fig. 1) that is situated directly in front of the delay

line, input A_1.

2.3 Hardware Specifications

Some specifications were already stated in Sections 2.1 and 2.2, notably those associated with the AO deflector, system frequencies and tuners.

2.3.1 AO Deflector, Acoustic Delay Line, and Delay Line RF Power Amplifier

The specifications related to the AO deflector were given in Section 2.1.2. In order to move the correlation peak to the center of the CCD array a delay equal to $T_{eff}/2 = 0.2$ μs must be introduced in the receiver input at antenna A_1, shown in Fig. 1. Because of losses, cable sections cannot be used, as high frequencies will be attenuated as much as 9 dB more than low frequencies, neither can SAW delay lines. The only choice is the bulk acoustic delay line, for instance, produced by Brimrose [53]. Again, because of losses the delay line must be accompanied by an RF amplifier to produce overall loss of 0 dB. Specifications for the bulk acoustic delay line and RF amplifier are:

Center frequency:	0.75 GHz
Bandwidth:	0.5 GHz
Delay:	0.2 μs flat over the bandwidth
RF amplifier:	when attached to the delay line to produce 0 dB overall loss over the bandwidth

2.3.2 Laser Diode, Intensity Modulation and Loaser Focussing Optics

The Spectra Diode Labs (SDL) laser diode with maximum optical power of 100 mW is recommended [25,37]. Following the instructions of the manufacturer a coaxial cable is introduced into the diode housing in order to product direct intensity modulation of the

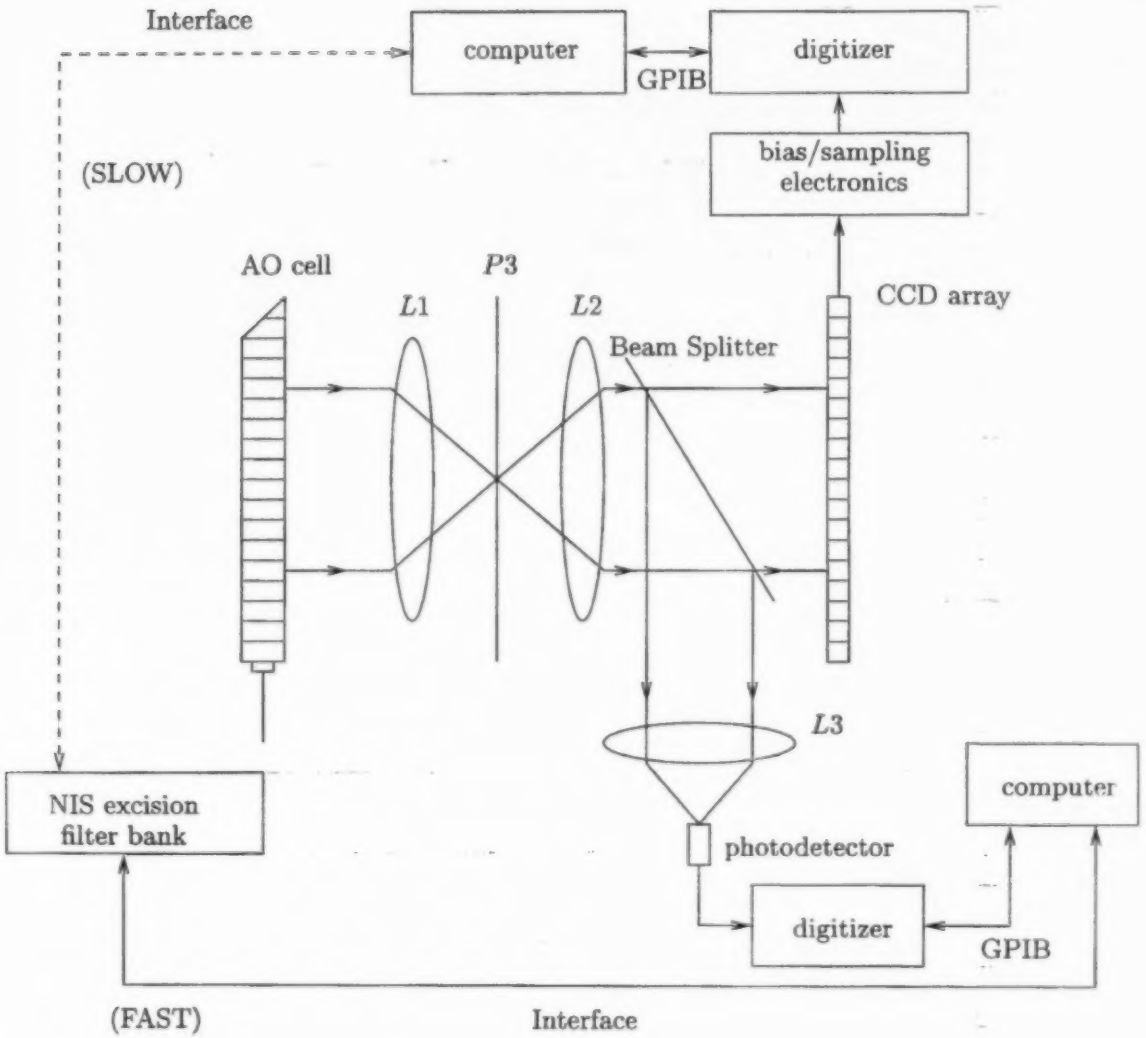

Figure 4: A space-integrating output for fast detection and excision of NIS, and CCD array time-integrating output for slow detection and excision of NIS.

diode, with RF signal of center frequency equal to 0.75 GHz and bandwidth equal to 0.5 GHz, as shown in Fig. 1. The alternative to direct modulation (which sometimes can be very noisy if the laser diode is not well chosen) is to perform the intensity modulation of the laser beam outside the laser diode by using, for instance, an acousto-optic modulator [1].

There are many off-the-shelf modules that can be used for the laser focussing optics [37]. The simplest one, for instance, is to use Newport Research Corporation 8.6 mm focal length lens (F-L20) followed by Melles Griot 01LCP136 cylindrical lens to produce a line illumination as optical input to the AO deflector.

2.3.3 Pre-Detection Optics and CCD Array at the Time-Integrating Output

Equations giving angle amplification of the two spherical lenses is given in Appendix II. The AO cell aperture is imaged by Melles Griot lenses 01LAO037 and 01LAO059. In addition, a cylindrical lens should be used, in between the last imaging lens and the detector, to match the optical beam to the height of the detector array [48].

A special CCD array was built [56] for the purposes of the AO time-integrating processor. In order to achieve a wide dynamic range, the array uses a nonlinear transfer curve between the optical input and the output voltage. The optical dynamic range achieved was 57 dB.

2.3.4 The Notching Adaptive Feedback Loop, Notch Filters, AGC and Space-Integrating Output

The notching feedback loop, shown in Fig. 4 is slow due to time integration at the CCD array. The space integrating output is fast and can be used for notching signals that have large amplitudes and are detectable with a single photodetector. It can also be used as an AGC, connected either to RF power amplifier of the acoustic delay line or to the AO deflector

driver. The bias/sampling electronics of the CCD array, digitizer and computer operated notch filter bank is well described in [37,25]. The digitally tuned notch filters were obtained from Pole/Zero Corporation [57]. The notch filters can have the center frequencies well into the GHz range.

2.3.5 Auxiliary Electronics

The only critical part in design of auxiliary electronics is the low single-sideband modulation (LSSM) module, shown in the Inset C in Fig. 1.

3 Application of Designed Processor to Signals with Strong Doppler Effect

The Doppler effect manifests itself on an electromagnetic wave of frequency ω and wavenumber k, that is emitted by a moving object at speed v, as increase or decrease the frequency, termed Doppler frequency $\omega_D = \omega \pm kv$ that is recorded by a stationary receiver of the electromagnetic wave. Consider an object moving at speed $v = 1000$ m/s, and assume frequency from low ESM range, say $\omega = 2\pi \times 3$ Grad/s, it follows that $\lambda = 0.1$ m and $k = 2\pi \times 10$ m^{-1}, and the Doppler shift will be $\mu = \pm kv = \pm 2\pi \times 10^4$ rad/s. Consider now the resolution required by the system in order to resolve 10 KHz frequency change at center frequency of 3 GHz. For a 500 MHz bandwidth AO deflector to obtain 10 KHz resolution we need time-bandwidth product of $TB = 500$ MHz/10 KHz $= 5 \times 10^4$. This is by an order of magnitude more that the present AO technology can deliver. Consider now the rate of change of the frequency. Let us assume that the moving object can accelerate as much as 10 G's, that is, $a \simeq 100$ m/s^2. Therefore the speed change from 0 to 1000 m/s can be accomplished in

10s. The Doppler frequency would change from 3 GHz to 3 GHz$\pm 10^4$ Hz. Thus, since the resolution of our system is 2.5 MHz, as computed in Section 2.1.2, even after 10s of time integration the processor would not be able to distinguish the frequency change.

4 Conclusions and Recommendations

With the available off-the-shelf AO components and RF components (such as tuners) it is possible to design an AO processor to cover the ESM band from 0.5 to 26.5 GHz with *almost real-time 100% interception* of LPI and other signals. The major hardware components as well as their manufacturers have been identified.

With further research effort it is possible to considerably improve the performance of the processor, by increasing its time-bandwidth product. The research effort should be directed into (a) studies of AO interaction in highly lossy acoustic medium, numerical modelling of the AO interaction with high acoustic losses, and simulation of the processor performance with predistorted input signals and (b) experimental investigation of the processor performance with predistorted input signals.

5 References

1. A. VanderLugt, *Optical Signal Processing*, Wiley, New York, 1992.

2. N.J. Berg and J.M. Pellegrino, Edts., *Acousto-Optic Signal Processing*, Marcel Dekker, New York, 1996.

3. H. Zmuda and E.N. Toughlian, Edts., *Photonic Aspects of Modern Radar*, Artech House, Boston, 1994.

4. A.D. Gantzoulis and D.R. Pape, Edts., *Design and Fabrication of Acousto-Optic Devices*, Marcel Dekker, New York, 1994.

5. T.P. Cheatham Jr. and A. Kohlenberg, "Optical filters – Their equivalence to and differences from electrical networks", *1954 IRE National Convention Record*, part 4, pp. 6-12.

6. E O'Neill, "Spatial filtering in optics", *IRE Transaction Inform. Theory*, Vol. IT-2, pp. 56-65, June 1956.

7. A.B. VanderLugt, "Signal detection by complex spatial filtering", *IEEE Trans. Inform. Theory*, vol. IT-10, pp. 139-145, April 1964.

8. S.R. Dashiell and A.A. Sawchuk, "Optical synthesis of nonlinear nonmonotonic functions", *Optics Communications*, vol. 15, pp. 66-70, September 1975.

9. L.M. Deen, J.F. Walkup and M.O. Hagler, "Representation of space-variant optical systems using volume holograms", *Applied Optics*, vol. 14, pp. 2438-2446, October 1975.

10. H. Barney, "Transversal filter", U.S. Patent 2,451,465, October 1948.

11. L.J. Cutrona, E.N. Leith, C.J. Palermo and L.J. Porcello, "Optical data processing and filtering systems", *IRE Trans. Inform. Theory*, vol. IT-16, pp. 386-400, June 1960.

12. H.R. Carleton, N.T. Maloney and G. Metz, "Collinear heterodyning in optical processors", *Proc. IEEE*, vol. 57, pp. 769-775, May 1969.

13. D.L. Hecht, "Acousto-optic device technique – 400 to 2300 MHz", *1977 Ultrasonics Symposium Proceedings*, pp. 721-725.

14. W.K. Pratt, *Digital Image Processing*, Wiley, New York, 1978.

15. B.J. Thompson, "Hybrid processing systems – An assessment", *Proc. IEEE*, vol. 35, pp. 62-76, January 1977.

16. "Ultrasonic spectrum analyzer", Rept. 202-1, Airborne Inst. Lab., Mineola, New York, April 1950.

17. L.B. Lambert, "Wide-band instantenous spectrum analyzers employing delay-line light modulators", *IRE International Convention Record*, vol. 10, pt. 6, pp. 69-78, 1962.

18. T.M. Turpin, "Time integrating optical processors", *SPIE Symposium on Real-Time Signal Processing*, San Diego, August 1978.

19. P. Kellman, "Detector integration acousto-optic signal processing", *Proc. 1978 Inter. Optical Computing Conference*, London, 1978.

20. L.B. Lambert, "Optical correlation", in *Modern Radars*, R. Berkowitz, Edt., John Wiley, New York, 1965.

21. L. Slobodin, "Optical correlation techniques", *Proc. IEEE*, vol. 51, p. 1782, December 1963.

22. L.B. Lambert, M. Arm and A. Aimette, "Electro-optical signal processors for phased array antennas", in *Optical and Electro-Optical Information Processing*, Tippet et al., Edts., MIT Press, Cambridge, pp. 715-748, 1965.

23. P. Kellman, "Time-integrating optical processing", *Ph.D. Dissertation*, Stanford University, 1979.

24. R.D. Griffin and J.N. Lee, "Acousto-optical wideband correlator system: Design, implementation, and evaluation", *Applied Optics*, vol. 33, no. 29, 10 October 1994.

25. V.M. Ristic, "Acousto-optic correlation investigation", *Final Report for Defence Research Establishment Ottawa*, Ottawa, Ontario, June 1997.

26. J. Erickson, "Linear acousto-optic filtering with heterodyne and frequency-plane control", *Ph.D. Dissertation*, Stanford University, Electrical Engineering Department, June 1981.

27. J. Erickson, "Optical excisor performance limits versus improved signal detection", *Proc. SPIE*, vol. 639, pp. 232-239, 1986.

28. J.N. Lee, N.J. Berg, M.W. Casseday and P.S. Brody, "High-speed adaptive filtering and reconstruction of broad-band signals using acousto-optic techniques", *Proc. 1980 Ultrasonics Symp. Proc.*, pp. 488-492, 1980.

29. P.J. Roth, "Optical excision in the frequency plane", *Proc. SPIE*, vol. 352, pp. 17-23, 1982.

30. G.W. Anderson, F.J. Kub, R.L. Grant, N.A. Papamicolaou, J.A. Modolo and D.E. Brown, "Programmable frequency excision and adaptive filtering with a GaAs.AlGaAs.GaAs heterojunction photoconductor array", *Optical Engineering*, vol. 29, no. 10, pp. 1243-1248, 1990.

31. R.W. Brandstetter and P.G. Grieve, "Excision of interference from radio signals by means of a recursive optical notching filter", *Optical Engineering*, vol. 29, no. 7, pp. 804-815, 1990.

32. R.N. Ward and A. VanderLugt, "Signal distortion in an adaptive excision system", *Optical Engineering*, vol. 31, no. 3, pp. 606-613, March 1992.

33. C.S. Anderson, A.F. Zwilling and M.C. Zari, "Wideband acousto-optic processor for ESM applications", *SPIE*, vol. 1704, pp. 10-18, 1992.

34. C. Anderson, A. Dorsett, S. Tepper, M. Zari, A. Filipov, E. Adler and J. Pellegrino, "Wideband acousto-optic correlator for an ESM receiver upgrade", *SPIE*, vol. 1958, pp. 60-70, 1993.

35. E. Adler, E. Viveiros, J. Mait, B. Berinato, A. Zwilling and N. Mohon, "Common module acousto-optic architecture for wideband signal processing", *SPIE*, vol. 1291, pp. 2-10, 1990.

36. E. Viveiros, E. Adler, M. Patterson, F. Elmer and D. Pak, "Demonstration of a wideband acousto-optic correlator in an ESM testbed", AMSRL-SS-1B, pp. 16-21, 1995 (unpublished).

37. A.M. Kiruluta, "Acousto-optic processors for the detection of spread-spectrum radar signals", *Ph.D. Dissertation*, University of Toronto, Department of Electrical and Computer Engineering, 1997.

38. N.A. Riza, "In-line interferometric time-integrating acousto-optic correlator", *Applied Optics*, vol. 33, no. 14, pp. 3060-3069, 10 May 1994.

39. N.A. Riza, "Coherent optical correlator with wideband signal processing capabilities", *Optical Processing and Computing*, p. 4, November 1993.

40. C.W. Keefer and M.J. Ward, "Modified interferometric in-line time integrating correlator", *SPIE*, vol. 2026, pp. 177-184, 1993.

41. N.A. Riza, "The in-line acousto-optic interferometer as a correlator and spectrum analyzer", *SPIE*, vol. 2026, pp. 130-135, 1993.

42. N.A. Riza, "Optically efficient interferometric acousto-optic architecture for spectrum analysis", *Applied Optics*, vol. 31, no. 7, pp. 3194-3196, 1992.

43. B. Tasic and V.M. Ristic, "Triple-product optical processor for analysis of pulse-repetition and carrier frequencies of radar signals", *Applied Optics*, vol. 34, no. 35, pp. 8144-8147, December 1995.

44. P. Kellman, "Time-integrating signal processing", *Optical Engineering*, vol. 19, no. 3, pp. 370-375, 1980.

45. T.R. Bader, P. Kellman and H.N. Shaver, "Time-integrating optical processing", Final Technical Report, Airforce Office of Scientific Research, July 1981.

46. D.C. Hartup and N.T. Rhodes, "Acousto-optic processor for carrier frequency and envelope modulation analysis", *SPIE*, vol. 1704, pp. 98-104, April 1992.

47. D.C. Hartup, W.T. Rhodes, H.F. Engler and A.K. Garrison, "Channelized time- and space-integrating acousto-optic processor", *SPIE*, vol. 1296, pp. 172-178, 1990.

48. V.M. Ristic, "Design and experimental investigation of two-dimensional acousto-optic processors for ESM applications", *Final Report for Defence Research Establishment Ottawa*, Ottawa, Ontario, March 1995.

49. J. Rhea, "New architectures and algorithms push DSP to the limit", *Military and Aerospace Electronics*, pp. 12-17, November 1996.

50. E. James Crascenzi Jr. and Roger D. Fields, "Miniature tuner serves diverse SIGINT applications", *Microwave and RF*, pp. 69-79, September 1995.

51. Watkins-Johnson Company, 3333 Hillview Avenue, Palo Alto, CA 94304-1223, "WJ-TN-170 Receiver", April 1995. (The tuner translates any 500 MHz bandwidth from 0.5 to 26.5 GHz to an IF output from 0.75 to 1.25 GHz.)

52. Condor System Inc., 2133 Samaritan Drive, San Jose, CA 95124, "Condor-TN-618-Tuner", June 1995.

53. Brimrose Corp., 5020 Campbell Blvd., Baltimore, MD 21236, USA.

54. A.M. Kiruluta, V.M. Ristic and J.P.Y. Lee, "Optical misalignment estimation in a time-integrated acousto-optic processor", *Optical Engineering*, vol. 36, no. 11, pp. 3028-3032, November 1997.

55. Sharp Microelectronics Technology, 5700 NW Pacific Rim Blvd., Camas, WA 98607. Processor BDSP9124DSP, 1998.

56. D. Smith, L. Harrison, J. Pellegrino and D. Simon, "Performance of high-dynamic range CCD arrays with various epi-layer structures", *SPIE*, vol. 1562, pp. 242-246, 1992.

57. Pole/Zero Corporation, 5530 Union Center Drive, West Chester, OH 45069.

6 Appendix I

Optical misalignment estimation in a time-integrating acousto-optic processor

Andrew M. Kiruluta
Velimir M. Ristic
University of Toronto
Acousto-Optic Research Laboratory
Applied Science and Engineering
Toronto, Ontario M5S 3G4
E-mail: ristic@ecf.toronto.edu

Jim P. Y. Lee
Defense Research Establishment Ottawa
Department of National Defense
Shirley's Bay, Ontario K1A 0Z4, Canada

Abstract. An acousto-optic time-integrating correlator with center frequency 80 MHz, bandwidth 40 MHz, time aperture 10 μs, and signal bandwidth 20 MHz was designed and assembled. A novel electronic method for estimating the overall optical misalignment in the processor was devised and tested. It represents a simple and robust alternative to purely optical procedures. The resolution accuracy of the method is limited by the CCD pixel dimensions. As a side result, the scaling law that applies to the output signal when using CCD detection is also derived.
© *1997 Society of Photo-Optical Instrumentation Engineers.* [S0091-3286(97)01411-6]

Subject terms: acousto-optics; time-integrating processors; radar.

Paper 11027 received Feb. 14, 1997; revised manuscript received June 11, 1997; accepted for publication June 16, 1997.

1 Introduction

Acousto-optic (AO) correlators promise small, lightweight processors for detecting and analyzing inherently wideband radar signals that are often corrupted by noise and narrowband interference signals (NISs).[1–4] As in all optical systems, the performance is greatly influenced by the level of component alignment in the system. Any slight misalignment in the system can lead to erroneous results and, most often, to a distorted output. Currently, a number of optical alignment evaluations systems exist on the market. These systems tend to be all-optical, bulky, and expensive. In this paper, we propose a robust, all-electronic approach to evaluating alignment issues in such systems. The method is developed on a time-integrating AO processor, but can easily be modified to work on other optical systems.

This correlator, of the electronic reference type,[5] is schematically shown in Fig. 1. The two signals to be correlated are frequency-shifted (insets A and B) and then applied to an appropriately biased laser diode and to the input of the AO cell. In designing the processor, the reference tone frequency f_c was placed at the lower cutoff frequency (f_l^{AO}) of the AO cell's passband, and the upper cutoff frequency (f_h^{AO}) of the signal bandwidth was placed at the upper cutoff frequency of the AO cell's passband, as shown in inset D of Fig. 1.

With this choice and a 40-MHz-bandwidth AO cell centered at 80 MHz, the other relevant frequencies are: the difference frequency $f_0 = 30$ MHz, the reference-tone frequency $f_c = 60$ MHz, and the intermediate frequency defined as $f_{if} = f_0 + f_c = 90$ MHz. The input signals $s_1(t)\cos(2\pi f_0 t)$ and $s_2(t)\cos(2\pi f_0 t)$ were modeled as pulsed radar cw signals as shown in insets A and B.

The intensity of the laser diode is

$$I_d(t) = A_1\{1 + m_1\ \mathrm{Re}[s_1(t)\exp(j\omega_0 t)]\}, \tag{1}$$

where A_1 is the dc bias amplitude, m_1 is the modulation depth, $s_1(t)$ is the bandpass signal of interest, and ω_0 is the modulation carrier frequency.

The intensity $I_{det}(t,\tau)$ imaged onto the CCD array is, by the multiplicative nature of intensity,

$$\begin{aligned} I_{det}(t,\tau) &= I_d(t)T_{eff}(t-\tau) \\ &= A_1\{1 + m_1\ \mathrm{Re}[s_1(t)\exp(j\omega_0 t)]\}\,\eta\,\frac{A_2}{2} \\ &\quad \times |1 + m_2 s_2^*(t-\tau)\exp[-j\omega_0(t-\tau)]|^2 \end{aligned} \tag{2}$$

where $T_{eff}(t-\tau)$ is the effective transmittance function of the AO cell, A_2 is the power of the signal applied to the transducer of the AO cell, η is the AO diffraction efficiency, and m_2 is the modulation depth the AO cell.

After detector integration it follows that

$$\begin{aligned} R(\tau) &= \int_0^{T_i} I_{det}(t,\tau)\,dt \\ &= \underbrace{\eta\,\frac{A_1A_2T_i}{2} + \eta\,\frac{A_1A_2m_2^2}{2}\int_0^{T_i}|s_2(t-\tau)|^2\,dt}_{\text{variable bias term (VBT)}} \\ &\quad + \eta\,\frac{A_1A_2m_1m_2}{2}\,\mathrm{Re}\left[\exp(j\omega_0\tau)\int_0^{T_i} s_1(t)s_2^*(t-\tau)\,dt\right], \end{aligned} \tag{3}$$

where T_i is the integration time, and $\tau = T/2 + x/v$, in which T is the AO cell delay time, x is the coordinate in the direction of the acoustic-wave propagation, and v is the acoustic velocity. Equation (3) can be written in compact form as

$$R(\tau) = \mathrm{VBT} + \eta\,\frac{A_1A_2m_1m_2}{2}\,|A_{12}(\tau)|\cos[\omega_0\tau + \phi_{12}(\tau)], \tag{4}$$

 © 1997 Society of Photo-Optical Instrumentation Engineers

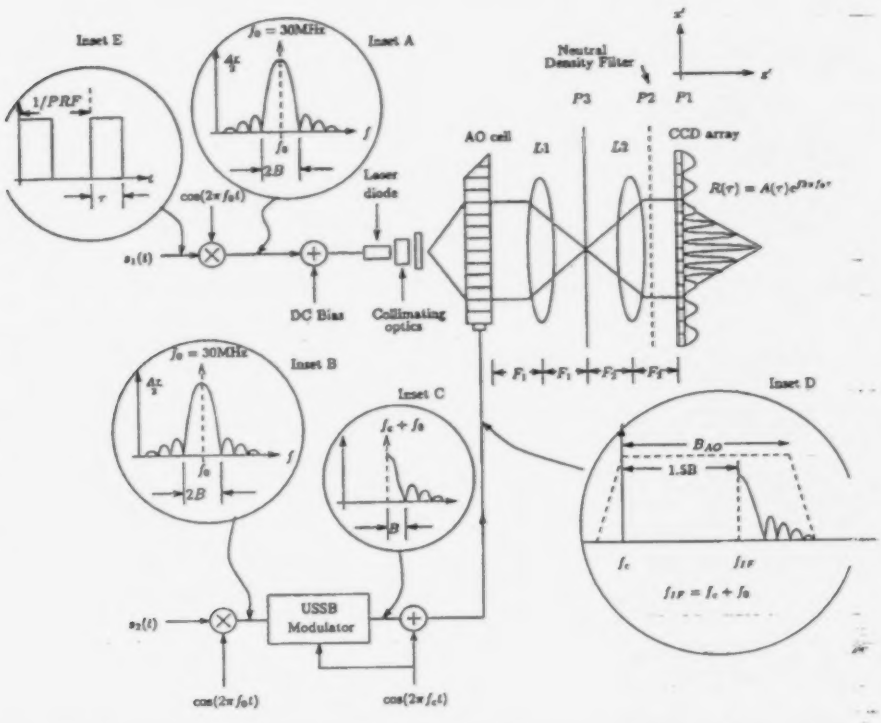

Fig. 1 Reference-tone AO processor for radar signal processing. Simulated radar signals $s_1(t)\cos(2\pi f_0 t)$ and $s_2(t)\cos(2\pi f_0 t)$ are introduced into the processor as shown. USSB is an upper single-sideband modulator that is used to translate the input signal to $f_c + f_0$ and to remove signal bandwidth redundancy by passing only the upper band as shown in inset C. $B = 20$ MHz is the signal bandwidth, and B_{AO} is the bandwidth of the AO cell.

where it is convenient to express the correlation function as[5]

$$\int_0^{T_i} s_1(t)s_2^*(t-\tau)\,dt = |A_{12}(\tau)|\exp[j\phi_{12}(\tau)]. \tag{5}$$

Several other terms appear in the integration given in Eq. (3). These terms, containing factors of $\cos(2\pi f_0 t)$ and $\cos(4\pi f_0 t)$, all integrate to zero for integration times T_i substantially longer than the difference period $1/f_0$. To move the correlation peak away from the edge of the AO cell to its optic center, as shown in Fig. 1, a delay of approximately $T/2 = 5\ \mu$s was applied to $s_1(t)$.

The focal length of both lenses $L1$ and $L2$ used in the system of Fig. 1 was 38.10 mm, providing for an overall magnification of $F_2/F_1 = 1$. The effective length of the AO cell is 6 mm; hence the minimum required CCD array length to match this aperture was $(F_2/F_1)\times 6$ mm. The CCD array used in this experiment had 2048 pixels, each of dimension $13\times 13\ \mu$m, and a readout rate of 10 MHz. This translates into a length of $13\ \mu\text{m}\times 2048 \approx 26.6$ mm, which is well above the minimum required.

2 CCD Scaling Law

Consider a sample output of a typical correlation of two pulses, each of duration t'. The total time duration of the correlation triangle in the detector plane is $2t'$. However, if we plot the correlation as a function of x, its duration x' will be dilated by a factor of v, the velocity of the acoustic wave in the AO cell. As well, other factors can contribute to the change in spatial dimension of the correlation: namely, the magnification of the imaging optics, equal to one in our case, and proper alignment of the cell aperture with the CCD detector array. This spatial correlation is sampled by the CCD pixels at a readout rate of 10 Mhz. With a correlation width of x', the number of pixels to cover this width is x'/δ, where δ is the length of each pixel in the array. The resulting width of the correlation in the time domain (as viewed on the oscilloscope) will thus be given by $t'' = x'/(10\ \text{MHz})\delta$. Since the CCD pixel dimension was $13\times 13\ \mu$m, it follows that $t'' = x'/130$. The original time correlation was mapped into the spatial domain through $2t' = x'/v$; hence, the observed correlation width t'' is related to the original time correlation by

$$t''=\frac{x'}{130}=\frac{2vt'}{130}=\frac{2\times(616\ \text{m/s})t'}{130}\approx 10t'. \tag{6}$$

Therefore, the observed correlation will have its base dilated by a factor of $10t'/2t'=5$ relative to the original.

3 Optical Misalignment Estimation

Using the results of the previous sections and a white Gaussian noise source, a procedure was devised to estimate the overall optical misalignment in the processor. Because white noise contains all frequencies in equal proportion, it is a convenient signal for system measurements, since it covers any chosen signal bandwidth fully.

Suppose that the signals $s_1(t)$ and $s_2^*(t-\tau)$ are replaced by a white Gaussian noise sample function $n(t)$ and its delayed version $n^*(t-\tau)$. The time-average correlation integral in Eq. (5) can be written as

$$\frac{1}{T_i}\int_0^{T_i} n(t)n^*(t-\tau)\mathrm{d}t$$

$$=\frac{1}{T_i}\int_{-\infty}^{\infty}|N(f,T_i)|^2\exp(j2\pi fT_i)\mathrm{d}f, \tag{7}$$

where a truncated sample segment of the noise process $n(t)$, defined over the integration range $0\leq t\leq T_i$, has short-time Fourier transform $N(f,T_i)$ given by

$$N(f,T_i)=\int_0^{T_i} n(t)\exp(-j2\pi ft)\mathrm{d}t. \tag{8}$$

If this white noise process is then passed through a bandpass filter of center frequency f_0 and quality factor Q, the spectral density S_N, for $Q\gg 1$, is given by[6]

$$S_N(f)\approx\begin{cases}\dfrac{N_0/2}{1+4Q^2(f-f_c)^2/f_c^2} & \text{for } f>0,\\[2ex] \dfrac{N_0/2}{1+4Q^2(f+f_c)^2/f_c^2} & \text{otherwise,}\end{cases} \tag{9}$$

and $N_0/2$ is the peak power spectral density.

The time-averaged correlation is thus given by

$$\hat{R}_N(\tau)=\frac{1}{T_i}\int_0^{T_i} n(t)n^*(t-\tau)\mathrm{d}t$$

$$=\mathcal{F}^{-1}\{S_N(f)\}=\frac{N_0T_i\pi f_0}{2Q}\exp\left(-\frac{|\tau|\pi f_0}{Q}\right), \tag{10}$$

where $\mathcal{F}^{-1}\{\cdot\}$ denotes the inverse Fourier transformation operator. Substituting the correlation function given by Eq. (10) in Eq. (4) yields

$$R_e(\tau)=\mathrm{VBT}+\eta\frac{A_1A_2T_im_1m_2}{2}\left[\frac{N_0\pi f_0}{2Q}\exp\left(-\frac{|\tau|\pi f_0}{Q}\right)\right], \tag{11}$$

where it is understood that the CCD discards the carrier information and hence $R_e(\tau)$ represents the envelope of the output plus bias.

3.1 *Experimental Verification*

A wideband white-Gaussian-noise generator was used to provide the input signals. A pair of bandpass filters with center frequency equal to the difference frequency $f_0=30$ MHz and bandwidth $B=50$ kHz for $Q=f_0/B=600$ provided inputs shown in insets A and B of Fig. 1. Such a high Q factor was chosen in order to sharpen the correlation response peak and provide a more accurate measurement of the misalignment error. Furthermore, for an arbitrary Q factor we have $S_N(f)=N_0/2[1+Q^2(f/f_c-f_c/f)^2]$, and its inverse Fourier transform $\hat{R}_N(\tau)=\mathcal{F}^{-1}\{S_n(f)\}$ cannot be expressed in closed form without a large-Q assumption as in Eq. (10). This is an important consideration, because the method proposed here requires the existence of a closed-form expression for $\hat{R}_N(\tau)$, which is then used to fit the experimental data and subsequently estimate the alignment error.

The resulting noise-only correlation data, after bias removal, were then fitted numerically with the correlation model given in Eq. (11) using a least-squares fit with Gauss-Newton optimization of the cost function. The residuals of the fitting function were then used to calculate the variance and confidence intervals of the fit. This error was partly attributed to the optical misalignment in the system, which introduced distortions in the correlation envelope and was estimated by mapping it to the spatial domain using the CCD scaling law given in Eq. (6).

However, additional factors, predominantly effects of the CCD trapezoidal spatial response, the system aperture function, and detector nonlinearities, also play a part in the size of this error. The aperture-function component is intrinsically tied to the overall processor misalignment problem and hence is assumed to be allowed for in the estimated displacement. The CCD trapezoidal spatial response will introduce errors in estimating the location of the correlation peak. This error was lumped together with other anomalies by fitting the data of a "perfectly" aligned system. The resulting fitting error was then assumed to include the spatial response effects and became the limiting value of the accuracy of this approach. More on this later.

For situations where the operating range of the processor includes the nonlinear regions of the CCD response curve, the output data must be compensated prior to the fitting. If $R(\tau)$ represents the correlation of signals $s_1(t)$ and $s_2(t)$, the CCD detector response is then given by $g[R(\tau)]$, where $g[\cdot]$ is the detector nonlinearity.[7] This amounts to a dynamic range compression of $R(\tau)$. In theory, if the nonlinearity is known and monotonic, then we may find its inverse $g^{-1}[\cdot]$, and the inverse can then be used to recover $R(\tau)$. CCD dynamic transfer plots are usually provided by the manufacturers, and the inverse $g^{-1}[\cdot]$ can readily be obtained from them to linearize the output. (Note that in most cases this step is unnecessary, as the CCD array is normally operated in its linear range, thus avoiding overdrive and saturation.) Once the nonlinearity has been re-

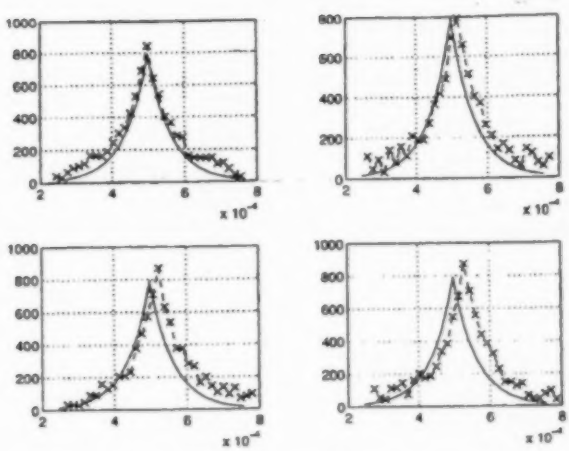

Fig. 2 Fit of the noise-only correlation data (represented by crosses) with the second term of Eq. (11). The estimated alignment error was: (a) 0.05 mm, (b) 0.3±0.05 mm, (c) 1.0±0.05 mm, (d) 1.2±0.05 mm. Horizontal axis: lag position in seconds; vertical scale: arbitrary.

moved, the correlation data are then fitted with the second term of Eq. (11) as shown in Fig. 2.

The error in estimating the displacement between the data and the fit along the τ axis was used to calculate the overall misalignment by mapping, using Eq. (6), its time-domain representation, as sampled by the oscilloscope, to its corresponding spatial-domain image while also compensating for the overall dimensional dilation relative to the original.

In the experiment, the laser-beam optical axis was varied with respect to the x' axis of the CCD plane $P1$ shown in Fig. 1. The amount of misalignment so introduced was found to be approximately equal to that from the fit estimates. This then becomes an independent check on the accuracy of the method. The correlation data, along with the corresponding fits for varying degrees of misalignments relative to the optical axis, are shown in Fig. 2. The various estimates of the misalignment errors, for varying laser-beam offsets from an established optical center, ranged from 0.05 to 1.2 mm.

In theory, the accuracy of this method is bounded by the degree of confidence in the fitting algorithm used and by the size of the pixels in the CCD array, which determines the spatial resolution. The array used in this work consisted of 13-μm-length pixels. Hence, we cannot resolve a misalignment less than this magnitude. The trapezoidal aperture response of the array sets this limitation. Figure 2(a) was used to estimate the accuracy of this method. In this case, the residual error was obtained by fitting the data for the best possible alignment of the laser beam. Hence, 50 μm is the best accuracy of the alignment error that can be obtained with this particular experimental setup. Thus, this becomes the uncertainty associated with all subsequent measurements.

4 Conclusions

A novel method for estimating the optical misalignment in an AO correlator has been demonstrated. The range of accuracy of the method is shown to be limited by the CCD pixel size and fitting accuracy of the algorithm adopted. In addition, the observed dilation in the time scale of the correlation width, attributed to the sampling characteristics of the CCD array, was studied and a mapping expression derived.

Acknowledgments

This research effort was jointly sponsored by the Defense Research Establishment Ottawa (DREO), the Natural Sciences Research Council of Canada (NSERC), and the Acousto-Optic Research Laboratory (AORL) of the University of Toronto.

References

1. W. T. Rhodes, "Acousto-optic signal processing: convolution and correlation," *Proc. IEEE* **69**, 65–79 (1981).
2. A. Vanderlugt, *Optical Signal Processing*, pp. 514–530, Wiley, New York (1992).
3. D. Hartup and W. Rhodes, "Acousto-optic processor for carrier frequency and envelope modulation analysis," *Proc. SPIE* **1704**, 98–104 (1992).
4. B. Tasic and V. M. Ristic, "Triple-product optical processor for analysis of pulse repetition and carrier frequencies of radar signals," *Appl. Opt.* **34**(35), 8144–8147 (Dec. 1995).
5. P. Kellman, "Integrating optical signal processing," *Opt. Eng.* **39** (3), 370–375 (1980).
6. S. Haykin, *Communication Systems*, pp. 291–292, Wiley, Toronto (1983).
7. B. M. Sadler and A. N. Filipov, "Integration of acousto-optic spectrum analyzers," in *Acousto-Optic Signal Processing*, N. J. Berg and J. H. Pellegrino, Eds., pp. 131–175, Marcel Dekker, New York (1996).

Andrew M. Kiruluta received a BEng in electrical engineering at Memorial University of Newfoundland (MUN) in 1991 and the MASc in biomedical engineering from the University of Toronto in 1992. In his master's degree thesis, he developed a system for predictive tracking of head and eye movements to generate a line of sight using adaptive Kalman filtering techniques. He subsequently took an assignment as a researcher engineer at the University of Toronto's Medical Biophysics Department, designing pulse sequences for a magnetic resonance imager. He is currently a PhD candidate with the Acousto-Optic Research Laboratory, Department of Electrical and Computer Engineering, at the University of Toronto. His research interests include acousto-optics, Fourier optics, photorefractive effects, and optical information processing for communication systems and medical imaging modalities.

Velimir M. Ristic received his PhD from Stanford University, is the Coordinator of the Acousto-Optic Research Laboratory, and is a professor of Electrical and Computer Engineering at the University of Toronto. The principal interests of Dr. Ristic's research group are experimental investigation and theoretical studies of optical processors, especially for radar and ir image processing; surface-acoustic-wave filter design and technology; and hybrid integrated optics communication devices and technology. He is a Fulbright and a Teslacholar.

Jim P. Y. Lee received the BSc degree with distinction from the University of Calgary, Calgary, Alberta, in 1975, the MASc degree from the University of Toronto, Toronto, Ontario, in 1977, and the PhD degree from Carleton University, Ottawa, Ontario, in 1986, all in electrical engineering. He joined the Defense Research Establishment Ottawa in 1977 as a defense scientist, where he has been engaging in the research and development of radar electronic-support-measures (ESM) receiving systems for EW applications. From 1980 to 1989, he was project leader responsible for the R&D of acousto-optic technology for EW applications. During this period, he developed and field-tested an acousto-optic radar ESM receiver and a 2-D acousto-optic receiver for simultaneous spectrum analysis and direction finding. He was also active in the development of IFM receiver technology and large-dynamic-range photodetector arrays. Since 1993, Dr. Lee has been the group leader of the Sensors Group. His current research interests include intrapulse signal-processing techniques, direction-finding and multipath effects, and LPI architectures and techniques. Dr. Lee serves as the IEEE/AESS technical editor for EW systems. He holds two patents and has published over fifty technical papers and reports on EW signal processing.

7 Appendix II

Acoust-Optic Research lab Note

ANGLE AMPLIFICATION WITH LENSES

The use of convex lens pairs, shown in Figure 1, is far superior to that of using prisms. The configuration shown is a 2 focal-length imaging system. Angle amplification is defined as the derivative of the output angle with respect to the input angle:

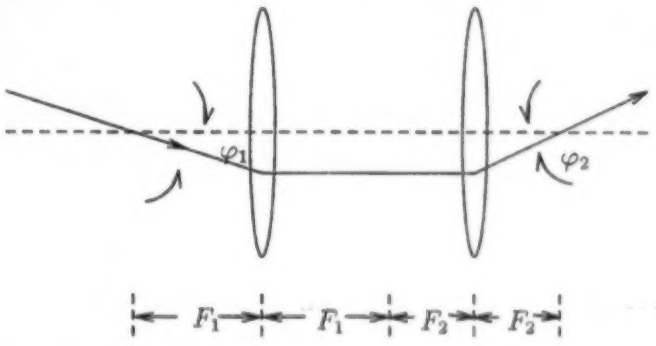

Figure 1: Pair of Concave Lens for Angle Amplification.

$$A = \frac{d\varphi_2}{d\varphi_1} \tag{1}$$

In terms of focal lengths and the input angle, the angle amplification is given by

$$A = \frac{F_1}{F_2} \frac{1}{cos^2(\varphi_1) + \frac{F_1}{F_2}\sin^2(\varphi_1)} \tag{2}$$

For small input angles, the amplification is approximately independent of input angle and is, to a good approximation, the ratio of the focal length of the first lens to that of the second lens

$$A \simeq \frac{F_1}{F_2} \tag{3}$$

The configuration shown in Figure 1 is very useful when it is needed to match two optical apertures with no loss to optical power as shown in Figure 2.

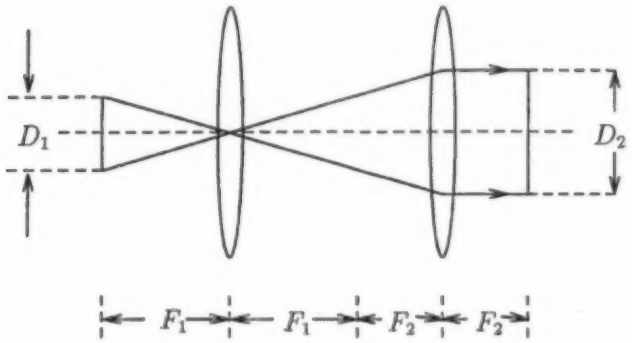

Figure 2: Matching Two Optical Apertures

In Figure 2, $A \simeq \frac{F_1}{F_2} \simeq \frac{D_2}{D_1}$. Here, we have assumed circular apertures. If one-dimensional amplification is needed, the configuration shown in Figure 2 can be combined with a single cylindrical lens at the output with $F_c = F_2$.

1. ORIGINATOR. (The name and address of the organization preparing the document) Organizations for whom the document was prepared. e.g. Establishment sponsoring a contractors report, or tasking agency are entered in Section 8. **V.M. Ristic, 523 Russel Hill Road, Toronto, Ontario M5P 2T2**	2. SECURITY CLASSIFICATION. (overall security classification of the document including special warning terms if applicable) **UNCLASSIFIED**

3. TITLE (the complete document title as indicated on the title page. Its classification should be indicated by the appropriate abbreviation (S, C or U) in parentheses after the title)

Design and Hardware Specifications for a 500-MHz Bandwidth Acousto-optic LPI Radar Correlator (U)

4. AUTHORS (Last name, first name, middle initial)

Ristic, Velimir M.

5. DATE OF PUBLICATION (month and year of publication of document)	6a. No. OF PAGES (total containing information, include Annexes, Appendices, etc.)	6b. No. OF REFS (total cited in document)
March, 1998	**34**	**57**

7. DESCRIPTIVE NOTES (The category of the document, e.g. technical report, technical note or memorandum). If appropriate, enter the type of report, e.g. interim, progress, summary, annual or final. Give the inclusive dates when a specific reporting period is covered.

FINAL REPORT

8. SPONSORING ACTIVITY (The name of the department project office or laboratory sponsoring the research and development. Include the address.

Defence Research Establishment Ottawa, 3701 Carling Avenue, Ottawa, K1A 0Z4

9a. PROJECT OR GRANT NO. If appropriate the applicable research and development project or grant number under which the document was written. Please specify whether grant of project. **Project 1410 SM 1ac11**	9b. CONTRACT NO. (If appropriate, the applicable number under which the document was written). **W7714-7-0118/001/SV**
10a. ORIGINATORS DOCUMENT NUMBER (The official document number by which the document is identified by the originating activity. The number must be unique to this document) **DREO/VMR - 1998** DREO CONTRACTOR REPORT 98-613	10b. OTHER DOCUMENT NUMBERS (any other number which may be assigned to this document either by the originator or by the sponsor.

11. DOCUMENT AVAILABILITY (any limitations or further dissemination of the document, other than those imposed by security classification)

(x) Unlimited distribution
( ) Distribution limited to defence departments and defence contractors; further distribution only as approved
( ) Distribution limited to defence departments and Canadian defence contractors; further distribution only as approved
( ) Distribution limited to government departments and agencies; further distribution only as approved
( ) Distribution limited to defence departments; further distribution only as approved
( ) Other (please specify)

12. DOCUMENT ANNOUNCEMENT (Any limitation to the bibliographic announcement of this document. This will normally correspond to the document availability (11). However, where further distribution beyond the audience specified on (11) is possible. A wider announcement audience may be selected.

As in 11, above.

13. ABSTRACT (a brief and factual summary of the document. It may also appear elsewhere in the body of the document itself. It is highly desirable that the abstract of classified documents be unclassified. Each paragraph of the abstract shall begin with an indication of the security classification of the information in the paragraph (unless the document itself is unclassified) represented as (S), (C), or (U). It is not necessary to include here abstracts in both offical languages unless the text is bilingual).

Hardware and system specifications for design and realization of an AO processor for ESM applications are discussed and recommended. The processor is to cover 0.5 to 26.5 GHz band with special emphasis on extraction of radar LPI signals. Further research efforts into the field of acousto-optic interaction, in presence of high acoustic attenuation, are also recommended with a goal of further ameliorating the existing processor design.

14. KEYWORDS, DESCRIPTORS or IDENTIFIERS (technically meaningful terms or short phrases that characterize a document and could be helpful in cataloguing the document. They should be selected so that no security classification is required. Identifiers, such as equipment model designation, trade name, military project code name, geographic location may also be included. If possible keywords should be selected from a published thesaurus. e.g. Thesaurus of Engineering and Scientific Terms (TEST) and that thesaurus-identified. If it is not possible to select indexing terms which are Unclassified, the classification of each should be indicated as with the title.)

acousto-optics, correlators, low probability of intercept(LPI), electronic surveillance receivers